Nuclear Instruments and Methods in Physics Research A 654 (2011) 88–96

Contents lists available at ScienceDirect

Nuclear Instruments and Methods in Physics Research A

journal homepage: www.elsevier.com/locate/nima

# Conceptual design and infrastructure for the installation of the first AGATA sub-array at LNL

A. Gadea [a,h,*], E. Farnea [b], J.J. Valiente-Dobón [a], B. Million [c], D. Mengoni [d,b,j], D. Bazzacco [b], F. Recchia [b], A. Dewald [e], Th. Pissulla [e], W. Rother [e], G. de Angelis [a], A. Austin [f], S. Aydin [b,t], S. Badoer [a], M. Bellato [b], G. Benzoni [c], L. Berti [a], R. Beunard [i], B. Birkenbach [e], E. Bissiato [a], N. Blasi [c], C. Boiano [c], D. Bortolato [b], A. Bracco [g,c], S. Brambilla [c], B. Bruyneel [e], E. Calore [a], F. Camera [g,c], A. Capsoni [c], J. Chavas [b], P. Cocconi [a], S. Coelli [c], A. Colombo [b], D. Conventi [a], L. Costa [a], L. Corradi [a], A. Corsi [g,c], A. Cortesi [c], F.C.L. Crespi [g,c], N. Dosme [o], J. Eberth [e], S. Fantinel [a], C. Fanin [b], E. Fioretto [a], Ch. Fransen [e], A. Giaz [g,c], A. Gottardo [d,b], X. Grave [k], J. Grebosz [n], R. Griffiths [f], E. Grodner [a], M. Gulmini [a], T. Habermann [l], C. He [a], H. Hess [e], R. Isocrate [b], J. Jolie [e], P. Jones [m], A. Latina [a], E. Legay [o], S. Lenzi [d,b], S. Leoni [g,c], F. Lelli [a], D. Lersch [e], S. Lunardi [d,b], G. Maron [a], R. Menegazzo [b], C. Michelagnoli [b], P. Molini [a], G. Montagnoli [d,b], D. Montanari [g,c,b], O. Möller [p], D.R. Napoli [a], M. Nicoletto [b], R. Nicolini [g,c], M. Ozille [i], G. Pascovici [e], R. Peghin [b], M. Pignanelli [g,c], V. Pucknell [f], A. Pullia [g,c], L. Ramina [b], G. Rampazzo [b], M. Rebeschini [b], P. Reiter [e], S. Riboldi [g,c], M. Rigato [a], C. Rossi Alvarez [b], D. Rosso [a], G. Salvato [b], J. Strachan [f], E. Sahin [a], F. Scarlassara [d,b], J. Simpson [f], A.M. Stefanini [a], O. Stezowski [q], F. Tomasi [c], N. Toniolo [a], A. Triossi [b], M. Turcato [b], C.A. Ur [b], V. Vandone [g,c], R. Venturelli [b], F. Veronese [b], C. Veyssiere [r], E. Viscione [c], O. Wieland [c], A. Wiens [e], F. Zocca [c], A. Zucchiatti [s]

[a] Istituto Nazionale di Fisica Nucleare, Laboratori Nazionali di Legnaro, Padova, Italy
[b] Istituto Nazionale di Fisica Nucleare, Sezione di Padova, Padova, Italy
[c] Istituto Nazionale di Fisica Nucleare, Sezione di Milano, Milano, Italy
[d] Dipartimento di Fisica dell'Università di Padova, Padova, Italy
[e] Institut für Kernphysik der Universität zu Köln, Köln, Germany
[f] STFC Daresbury Laboratory, Daresbury, Warrington WA4 4AD, United Kingdom
[g] Dipartimento di Fisica dell'Università di Milano, Milano, Italy
[h] IFIC, CSIC - Universitat de València, Spain
[i] GANIL, CEA/DSM-CNRS/IN2P3, Caen, France
[j] University of the West of Scotland, Paisley, UK
[k] Institut de Physique Nucléaire d'Orsay, CNRS/IN2P3, Université Paris Sud, Orsay, France
[l] GSI Helmholtzzentrum für Schwerionenforschung mbH, Darmstadt, Germany
[m] Department of Physics, University of Jyväskylä, Jyväskylä, Finland
[n] The Niewodniczanski Institute of Nuclear Physics, Polish Academy of Sciences, Cracow, Poland
[o] Centre de Spectrométrie Nucléaire et de Spectrométrie de Masse, CNRS/IN2P3, Université Paris Sud, Orsay, France
[p] Institut für Kernphysik, TU Darmstadt, Darmstadt, Germany
[q] IPN Lyon, IN2P3-CNRS, Université C Bernard Lyon-1, Villeurbanne, France
[r] DSM/DAPNIA, CEA/Saclay, Saclay, France
[s] Istituto Nazionale di Fisica Nucleare, Sezione di Genova, Genova, Italy
[t] Department of Physics, Faculty of Science and Art, Aksaray University, Aksaray, Turkey

The AGATA and PRISMA Collaborations

ARTICLE INFO

*Article history:*
Received 3 February 2011
Received in revised form
31 May 2011
Accepted 1 June 2011

ABSTRACT

The first implementation of the AGATA spectrometer consisting of five triple germanium detector clusters has been installed at Laboratori Nazionali di Legnaro, INFN. This setup has two major goals, the first one is to validate the γ-tracking concept and the second is to perform an experimental physics program using the stable beams delivered by the Tandem–PIAVE-ALPI accelerator complex. A large

* Corresponding author at: Instituto de Física Corpuscular (IFIC), CSIC-Universitat de València, Spain.
*E-mail address:* gadea@ific.uv.es (A. Gadea).

0168-9002/$ - see front matter 
doi:10.1016/j.nima.2011.06.004

Available online 15 June 2011

*Keywords:*
AGATA
PRISMA spectrometer
DANTE heavy-ion detector
HELENA multiplicity filter
Cologne plunger
TRACE Si detector

variety of physics topics will be addressed during this campaign, aiming to investigate both neutron and proton-rich nuclei. The setup has been designed to be coupled with the large-acceptance magnetic-spectrometer PRISMA. Therefore, the in-beam prompt $\gamma$ rays detected with AGATA will be measured in coincidence with the products of multinucleon-transfer and deep-inelastic reactions measured by PRISMA. Moreover, the setup is versatile enough to host ancillary detectors, including the heavy-ion detector DANTE, the $\gamma$-ray detector array HELENA, the Cologne plunger for lifetime measurements and the Si-pad telescope TRACE. In this paper the design, characteristics and performance figures of the setup will be described.



## 1. Introduction

The first implementation of the AGATA array [1–4] will operate at the INFN-Laboratori Nazionali di Legnaro (LNL). The installation at LNL has two main goals, to validate the $\gamma$-tracking concept and to perform an experimental campaign with the stable beams delivered by the Tandem-ALPI and the PIAVE-ALPI accelerator complex [5,6]. After the commissioning period, the experimental campaign will use five triple clusters of AGATA [7] (from now on referred as AGATA sub-array) coupled to the PRISMA [8] magnetic spectrometer. The AGATA sub-array replaces the previous $\gamma$-ray detector array CLARA [9]. The setup has been mainly designed to perform structure studies of moderately neutron-rich nuclei populated by grazing reactions as multi-nucleon transfer or deep-inelastic collisions. However, the AGATA sub-array can be used with other reactions, like for example Coulomb excitation, direct and fusion-evaporation reactions, and can be coupled to other complementary detectors. As it was mentioned above the AGATA sub-array installation at LNL has a double aim: an experimental campaign and the evaluation of the AGATA performance figures. However, the latter one is a challenging process that requires detailed analysis and, therefore, deserves dedicated publications. The first commissioning that evaluates the position resolution of the array has been published by Söderström and collaborators [10], other preliminary results can be found in Refs. [11–14]. The present manuscript will concentrate on a full description of the infrastructures associated with the AGATA sub-array at LNL including the complementary devices as well as the simulations to show the performance of the AGATA sub-array.

## 2. Nuclear structure studies using grazing reactions

High-resolution spectroscopy of neutron-rich nuclear species plays a major role for the understanding of nuclear structure at large isospin values. Topics of special interest for the present campaign are the evolution of the nuclear effective interaction in the monopole and multipole terms, the quenching of the known shell gaps and the development of new ones, the evolution of the nuclear collectivity and the shape phase transitions at large isospin values. Experimentally, these questions can be studied by exploring the nuclear spectrum up to medium-high-angular momentum and by direct measurement of transition probabilities. These topics represent an important part of the scientific programs of present and next generation radioactive beam facilities that will open new possibilities by going further away from the valley of stability. Nevertheless, moderately neutron-rich nuclei can be populated at medium- or high-angular momentum by transferring nucleons (neutron-pickup and proton-stripping being the projectile-like the nuclei of interest) in grazing reactions. Multi-nucleon transfer reactions and deep-inelastic collisions have been used with success in the last years to study the structure in the neutron-rich side of the nuclear chart. In the 1980's, Guidry and coworkers [15] suggested the possibility to populate high spin states in transfer reactions induced by heavy projectiles and in the 1990's Broda and collaborators performed pioneering work with large $\gamma$-detector arrays [16,17]. These early techniques were purely based on the measurement of $\gamma-\gamma$ coincidences between unknown transitions of the neutron-rich nucleus and known ones of the reaction partner. In recent years, the first dedicated setup for spectroscopy based on grazing reactions, in particular for medium mass or heavy neutron-rich nuclei, was developed, consisting on the CLARA array coupled to the PRISMA magnetic spectrometer [9]. This setup, as well as the present AGATA implementation coupled to PRISMA, aims at measuring in-beam prompt $\gamma$-rays detected with the Ge array in coincidence with the reaction product seen by the PRISMA spectrometer. This enables transitions to be assigned to the emitting nucleus by measuring the mass $A$ and atomic number $Z$ of the reaction products. The experimental activity at the CLARA-PRISMA setup has provided relevant spectroscopic information in various regions of the neutron-rich side of the Segrè Chart, that span from $N=24$ [18,19], $N=32$ [20], $N=40$ [21–23], up to $N=50$ [24]. In addition, a method for lifetime measurements, the Recoil Distance Doppler-Shift (RDDS), was developed for nuclei produced in multinucleon-transfer reactions in combination with a magnetic spectrometer [25–27]. This method will greatly benefit from the implementation of the AGATA sub-array, as it will be discussed later in this manuscript. The AGATA sub-array has now replaced CLARA at the target position of the PRISMA spectrometer; the higher efficiency and sensitivity of the new array with respect to CLARA will extend the studies of neutron-rich nuclei to more exotic species, giving the possibility of contributing to the understanding of the nuclear force at even larger isospin values.

## 3. The AGATA sub-array setup coupled to the PRISMA spectrometer

The setup at LNL includes two basic instruments, the AGATA sub-array and the PRISMA spectrometers. The design of the infrastructures and instrumentation has been largely conditioned by the coupling of these two instruments. In the next section a brief description of the AGATA sub-array and the PRISMA spectrometer will be given.

### 3.1. The first implementation of the AGATA spectrometer

The Advanced GAmma Tracking Array (AGATA) [1–4] is based on the novel concepts of pulse shape analysis [28–31] and $\gamma$-ray tracking [32–34] with highly segmented Ge semiconductor detectors. The AGATA sub-array being installed at LNL consists of five triple cluster elements, see Fig. 1. Given the number of elements, the optimal geometry of the array for the experimental activity foreseen at LNL is the compact distribution of the 15 Ge crystals arranged in the mentioned five triple clusters. This sub-array of AGATA is placed symmetrically along the optical axis of the

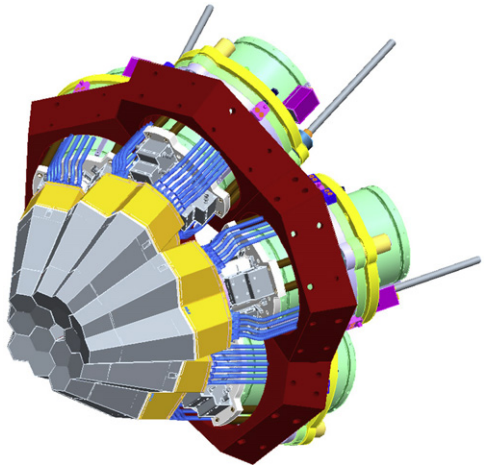

**Fig. 1.** Schematic view of the AGATA sub-array showing the five triple clusters (color online).

PRISMA spectrometer at approximately 180°. This is the optimal position to minimize the Doppler broadening. The full AGATA $4\pi$ geometry is based on 180 detectors, i.e. 60 AGATA triple clusters. The present AGATA sub-array is only 1/12 of the total and, as a consequence of the limited solid-angle coverage, other target-to-detector distances (referred from the target position to the surface of the detector), closer than the nominal 235 mm AGATA inner radius, can be also used. The effect of this reduced target-to-detector distance from the $\gamma$-ray emitting source translates into a larger efficiency (a factor of 2 for 145 mm) without significant losses in the resolution and peak-to-total performance [35], for reactions with low $\gamma$-ray multiplicity, in particular the already mentioned multi-nucleon transfer processes. More details on the performance figures of the array coupled to PRISMA will be given in Section 6.1.

### 3.2. The PRISMA magnetic spectrometer

PRISMA is a large-acceptance magnetic spectrometer designed to work with grazing reactions with the heavy-ion beams provided by the LNL accelerator complex. The basic characteristics of PRISMA are described in Ref. [8]. For the following discussion it is relevant to mention that PRISMA uses ion-tracking position-sensitive detectors to achieve the mass resolution. The tracking detectors provide the basic information to obtain the trajectory and velocity of the reaction products. According to the Monte Carlo simulations, up to velocities of approximately $v/c=10\%$, the intrinsic AGATA detector resolution is almost fully recovered if the recoil velocity is measured with a relative precision better than 1%, and if the recoil velocity direction is measured with an angular precision better than 1°. These values are actually well within the capabilities of PRISMA. A more detail discussion will be given in the Monte-Carlo simulation (Section 6.1).

## 4. Description of the setup installation

The sub-array of AGATA coupled to the PRISMA spectrometer is placed onto a platform that rotates from 0° to 117° with respect to the beam direction. Both devices are fixed on the platform and are located face-to-face in such a way that independently of the spectrometer angle selected for an experiment, the recoils that enter into the PRISMA spectrometer will have a trajectory of approximately 180° with respect to the central axis of the AGATA sub-array. The rotation and translation of AGATA produces tight constraints on the mechanical support, beam line and reaction chamber as well as to the liquid nitrogen cryogenic distribution lines. In this section the different mechanical aspects that characterize the AGATA and PRISMA setup will be discussed. The mechanical constraints of the setup limit further the use of the angular range mentioned above and therefore a final subsection will provide the angles available for the experiments.

### 4.1. Mechanical support

A stringent requirement of AGATA design is that the triple cluster elements should be mounted with a separation distance between them of 0.5 mm. Therefore, the use of bespoke designed AGATA structural flanges is compulsory. A subset of 15 flanges covering $1\pi$ sr has been used to allow the mounting of up to 15 AGATA triple clusters as well as other complementary $\gamma$-ray detectors. The main mechanical support, see Fig. 2, has been designed to enable the positioning of the AGATA flanges at the target position of the PRISMA spectrometer. The full structure is mounted on a translating frame to set the target-to-detector distance as well as allowing access to the area of the reaction chamber. This frame is placed on a rotating platform solidly linked to the PRISMA spectrometer. Therefore, the described mechanical structure allows the rotation and translation of the AGATA sub-array.

### 4.2. Beam line and reaction chamber

The beam line has been constructed in such a way that it can be held at two positions, see Fig. 3. The beam line retracts in order to rotate the array without any obstacle, from the AGATA support or the detectors. Once PRISMA and the AGATA sub-array have been placed at the desired angle, the beam line is extended to couple to the reaction chamber.

The beam line is formed of two concentric cylinders of different diameters that slide one within the other. The contact between the two cylinders is made with Teflon in order to have less mechanical stress between them. The high vacuum is ensured via an O-ring seal. The coupling of the beam line and the reaction chamber is made via a bellows with KF25 standard flanges. The design and construction of the reaction chamber has been motivated by the following bench marks: low $\gamma$-ray absorption, coupling to the existing PRISMA support, PRISMA rotation angle from 0° to 117°, versatility for positioning detectors inside the

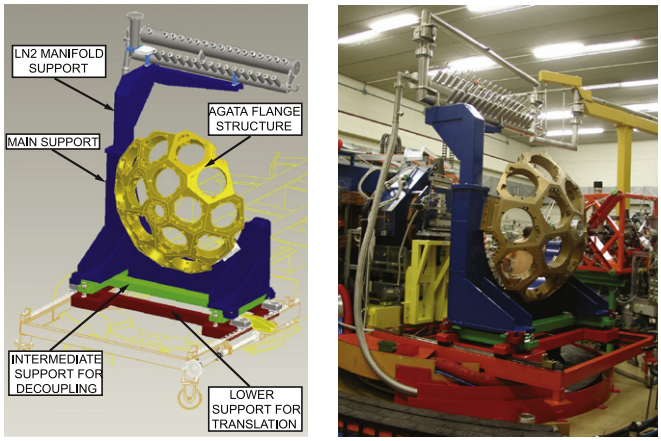


**Fig. 2.** A design drawing and a photograph of the mechanical support for AGATA at LNL, where a subset of 15 flanges covering $1\pi$ sr is shown. The interface between the lower and intermediate support allows the translation of the main support.

chamber and the necessity of a beam dump to decrease the γ-ray background directed toward the unshielded AGATA detectors. The result has been a 2 mm-thick spherical aluminum reaction chamber coupled directly to the chamber hosting the PRISMA Micro Channel Plate (MCP) entrance detector [36] with an angular range coverage from 0° to 117° and with an extended heavily shielded triangle-shaped chamber that can be used as beam dump as well as a versatile chamber to place detectors, feed-throughs, etc. The chamber presents three main parts (see Fig. 4): the main spherical body with an inner radius of 12 cm, the extended beam dump chamber and three spherical shells that all fit together form a vacuum seal for the chamber to operate at a ranges of rotation angles. The reaction chamber can host the DANTE detector, see Section 5.1, the TRACE detector Si-array, see Section 5.4, as well as the Cologne differential plunger, see Section 5.3. Moreover, the chamber is versatile enough to include a range of other complementary detectors.

### 4.3. Cryogenic basic infrastructures

The liquid nitrogen ($LN_2$) distribution system at the AGATA–PRISMA setup consists of the incoming vacuum isolated $LN_2$ line, the distribution and collector manifolds and the exhaust line for the liquid nitrogen and gas. Fig. 2 shows the $LN_2$ system and all its parts as mentioned above. The incoming line, used previously during the CLARA project, accommodates the rotation and translation of the array through specially designed *Johnston* joints. The distribution manifold is vacuum isolated and allows the connection of up to 15 AGATA triple clusters. The manifold collector, rigidly connected to the support structure of the array, was designed in order to comply with the safety regulations whereby the surplus (gaseous and liquid nitrogen) produced during the filling cycle are evacuated outside the building.

The manifold collector is connected to the exhaust line via a flexible vacuum hose running through a dedicated flexible cable tray (cable chain) used by AGATA and PRISMA cabling infrastructure. The presence of the exhaust line required the installation of non-return cryogenic valves in the out-gassing line of each single AGATA triple cluster.

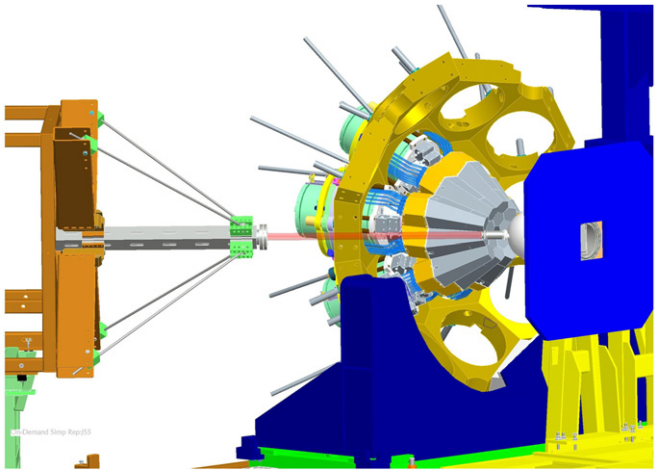

**Fig. 3.** Telescopic beam line for the AGATA–PRISMA setup. The beam line can be retracted back as well as extend to the nominal position to be coupled to the reaction chamber.

### 4.4. Available range for grazing angles

The reaction chamber itself is planned to allow the rotation of PRISMA in a broad angular range from 0° to 117°. Nevertheless, because of the mechanical support of AGATA and the beam line configuration there are some restrictions in the available angular range. The 0° configuration can only be used for an AGATA germanium to target distance of at least 243 mm. The AGATA nominal distance from the target is 230 mm, which is 235 mm from the germanium crystals. On the other hand, because of the radius of the reaction chamber, the closest possible AGATA sub-array to target distance is 140 mm, i.e. 145 mm from the germanium crystals. The thickness of the central pentagonal flange of the main mechanical structure prevents the use of grazing angles below 15° for the nominal distance. Due to the possible clashes between the beam line bellows and the AGATA clusters, the use of a grazing angle from 14° to 22° (closer target-AGATA distance: from 15° to 31°) requires that both flanges nos. 3 and 4 (see Fig. 5) must be empty while in the case of a grazing angle between 22° and 29° (closer target-AGATA detector distance: 32°) only flange no. 3 must be empty. Due to the thickness of flange no. 3, grazing angles between 29° and 37° (closer target-AGATA distance: 33° and 41°) are not available. Finally all angles between 37° and 117° (closer target-AGATA distance: 41° and 117°) are available with the five clusters of the AGATA placed in the five inner flanges of the mechanical support and with the beam dump placed on one of the planned supports inside the reaction chamber.

Table 1 summarises the angular ranges.

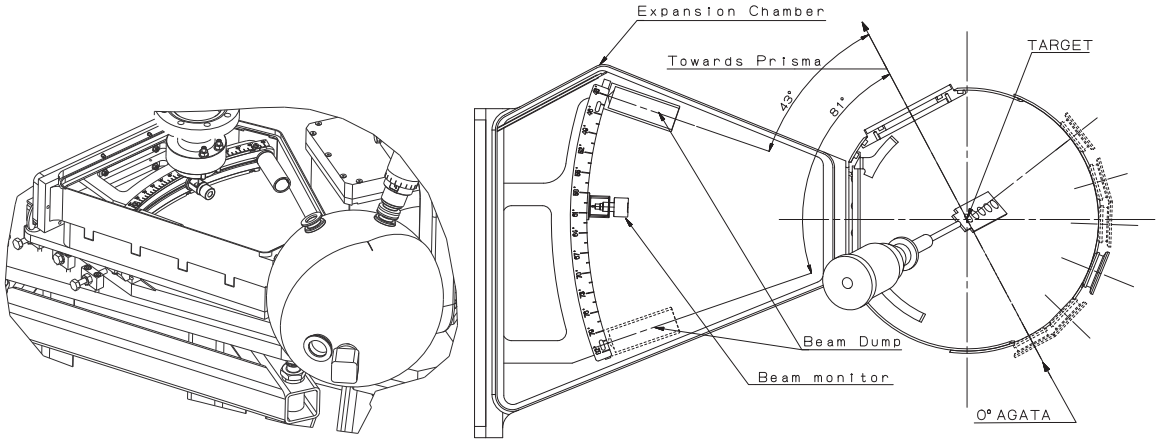


**Fig. 4.** Schematic side view (left) of the AGATA reaction chamber and the heavily shielded extended triangular-shaped chamber to be used as beam dump as well as a versatile chamber to place detectors. Horizontal cut (right) of the reaction chamber showing simultaneously different beam-input configurations.

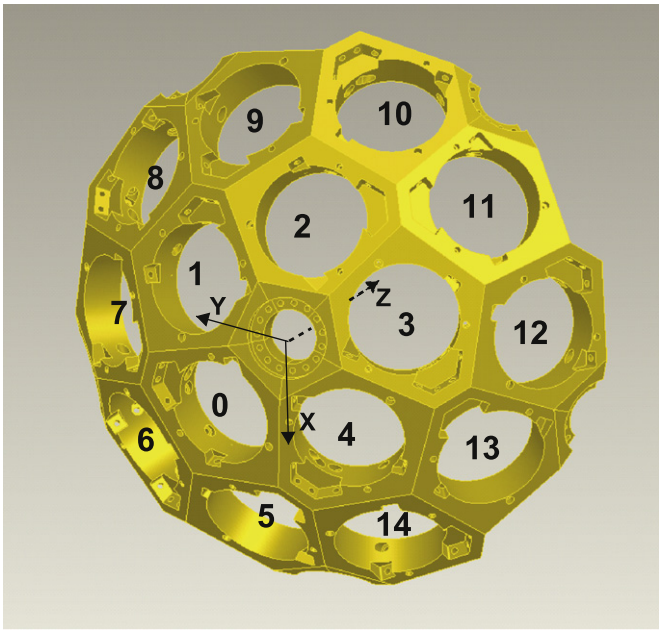


**Fig. 5.** Schematic view of the AGATA detector flanges with the numbering scheme, see text for more details.

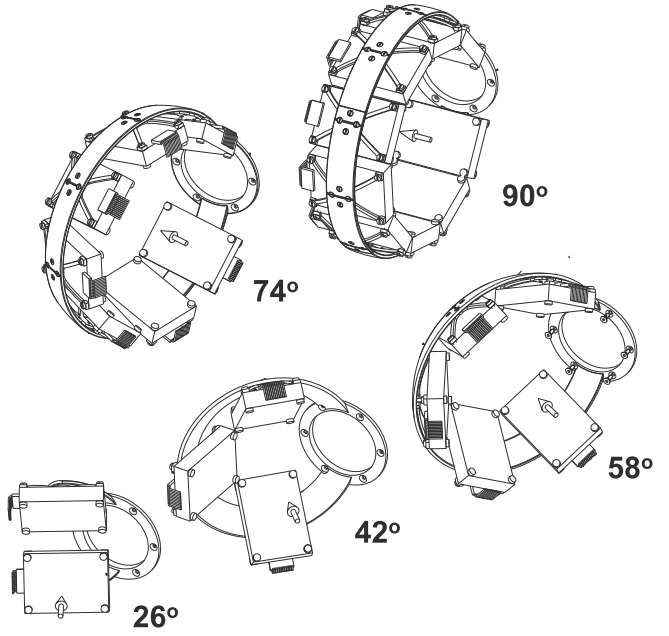


**Fig. 6.** Mechanical setup for the different angles of the DANTE array. The angles quoted in the figure refer to the nominal central position of the DANTE detectors with respect to the beam axis.

**Table 1**
Angular ranges available for the nominal distance (235 mm) and the closest possible distance (145 mm). The distance is referred from the center of the array up to the germanium crystal. The 0° angle is only possible at 243 mm from the germanium crystals. See text for details.

| Distance (mm) | Angular ranges | | | | |
|---|---|---|---|---|---|
| | Not available[a] | Available[b] | Available[c] | Not available[d] | Available[e] |
| 235 | 0–14° | 14–22° | 22–29° | 29–37° | 37–117° |
| 145 | 0–15° | 15–31° | 32° | 33–41° | 41–117° |

[a] Due to the thickness of central pentagon.
[b] If flanges 3 and 4 are empty.
[c] If flange 3 is empty.
[d] Due to the thickness of flange 3.
[e] Five AGATA triple clusters mounted.

## 5. The AGATA sub-array complementary instrumentation

Additionally to the PRISMA spectrometer, a number of complementary detectors can be used with the AGATA sub-array at LNL to perform the physics campaign. Two of them are considered to be an integral part of the setup, the heavy-ion position-sensitive detector array DANTE and the γ-ray multiplicity filter HELENA. In addition, a differential plunger for lifetime measurements, designed at Cologne University specifically for use at the grazing angle, and modules of the TRACE Si-PAD detector array, will be available for the physics campaign. In the following a brief description of these complementary devices will be given.

### 5.1. The heavy-ion detector DANTE

DANTE is a general purpose heavy-ion position-sensitive detector array based on MCP [37,38] that can be installed in the reaction chamber of the AGATA–PRISMA setup. The configuration of the single elements of DANTE is very similar to that of the start detector of the PRISMA spectrometer [36] and of the CORSET-type detector [39].

Each detector consists of a Mylar foil, at the entrance, for electron production, followed by two Micro-Channel-Plates (MCP), of dimensions $40 \times 60\ mm^2$, mounted in Chevron configuration. This detector allows the coverage of a large surface approximately $40 \times 60\ mm^2$ and provides three parameters, *X*, *Y* and time. The position and time resolution of DANTE is 1 mm and around 130 ps, respectively.

The final design of the DANTE array aims at maximizing the detection efficiency for the reaction products in combination with the γ-rays measured with the AGATA sub-array. As a consequence, the MCP detectors will be placed around the grazing angle, where the reaction cross-section is largest. Fig. 6 shows the different DANTE configurations for the various angles. The arrangement of the detectors in the array is flexible in order to place them at the grazing angle of the various reactions of interest.

### 5.2. The γ-ray detector array HELENA

HELENA is a detector array built out of 27 scintillation detectors based on 3 in. × 3 in. hexagonal $BaF_2$ crystals. These detectors are placed at 150 mm from the target, in five groups of eight, eight, four, four and three detectors each, to cover the maximum available space between AGATA and the PRISMA spectrometer, see Fig. 7. The solid-angle coverage is approximately 25% of 4 π with an overall full energy peak efficiency of 16% at 500 keV. The HELENA array is used both as a time reference and a multiplicity filter for γ-rays. The fast component of this scintillator gives to the HELENA array an excellent time resolution of around 600 ps. This allows for an essentially perfect separation between neutrons and γ-rays. Moreover, the dependence of the relative intensities of the two scintillation components of the $BaF_2$ (220 and 320 nm) on the type of interaction permits a discrimination against the internal radioactivity by analysis of the pulse shape. The pulse shape analysis is also an useful additional veto against pile up events. The multiplicity filter information will be used at first to disentangle direct reactions with low γ-ray multiplicity from the fusion-evaporation ones, with higher γ-ray multiplicity. A measurement of the total

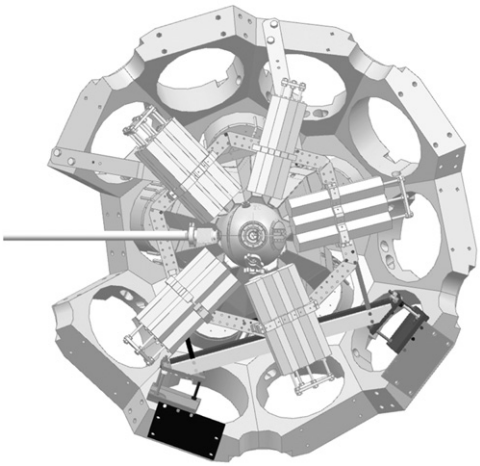

**Fig. 7.** Schematic view of the HELENA multiplicity filter within the AGATA flanges frame.

energy deposited may also be performed. See Refs. [40,41] for more detailed information. The HELENA mechanical support, attached to the main frame of the AGATA array, has been designed to allow for the maximum detection efficiency in the various detector configurations to ensure that individual HELENA detector groups can be extracted to leave space for additional AGATA triple clusters. One of the upper groups can be mounted in two possible locations to be compatible with the target-holder positions necessary for the use of the different DANTE detector angular configurations. Due to the fact that the AGATA sub-array may be used in any position between the nominal inner radius of 235 mm and the minimum inner radius of 145 mm, the HELENA individual supports include translation sliders that allow the HELENA detectors to be correctly centered around the target.

### 5.3. The Cologne plunger for grazing reactions

To open the possibility of Recoil Distance Doppler-Shift measurements, following the population of nuclear excited states in multi-nucleon transfer and deep-inelastic reactions at grazing angles, a dedicated differential plunger device [42] has been designed and built at the University of Cologne. In multi-nucleon transfer and deep-inelastic reactions the recoiling nuclei of interest leave the target in a direction which is normally different from the direction of the incident beam. The plunger device has to be oriented parallel to the recoil axis that means that the degrader foil of the plunger has to be moved along this axis. This fact requires a design that enables a rotation of the device with respect to the beam axis. Thereby the target center is kept fixed on the beam axis. The recoil axis coincides with the entrance axis of the PRISMA spectrometer which has the consequence that the plunger device follows exactly any rotation of the PRISMA spectrometer.

These considerations led to the design that is schematically shown in Fig. 8. All vital device components like the motor, a piezo-crystal used for a feed-back system and two inductive transducers for measuring the target–degrader separation have to be housed inside the target chamber. This is different from the concept followed for the standard Cologne-coincidence-plunger [43] where most of these components are located in a separate housing up-stream of the target chamber in order to minimize the amount of material by which the gamma radiation of interest could be absorbed on its way from the target to the surrounding germanium detectors. A compromise made whereby the necessary components were placed in a plane below the target and

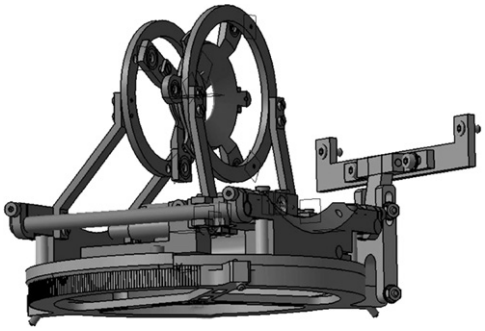

**Fig. 8.** Drawing of the plunger device and its supporting structure to be used in the AGATA reaction chamber.

**Table 2**
Specifications of the Cologne differential plunger for the use in grazing reactions.

| | |
|---|---|
| Target–degrader separation | 0–10 mm |
| Precision of the target–degrader separation setting (motor) | 0.1 μm |
| Inductive transducer resolution | 0.01 μm (0–40 μm range), 0.1 μm (0–200 μm range), 1 μm (0–5 mm range) |
| Maximum rotation respect to the beam axis | 60°[a] |

[a] The maximum angle can be increased to 70° by using different degrader cones and holding structures.

degrader holding structures in such a way that the solid angles covered by the PRISMA entrance acceptance and the AGATA spectrometer are kept free. The complete plunger device can be dismounted as a single unit from the target scattering chamber. A dedicated mechanical structure fixed inside the target chamber guarantees a precise positioning of the target in the pivot point of the experimental setup. In addition this structure allows for defined rotations with an angular accuracy of 0.5°. Some technical details are given in Table 2.

Like other Cologne plunger devices, this plunger setup is equipped with an active separation stabilizing system [44], which ensures a separation accuracy of about 1% between the target and degrader. The plunger device has been successfully used in a lifetime measurement performed at GANIL, France [45] in combination with the VAMOS [46] spectrometer and the EXOGAM [47] Ge detector array.

### 5.4. TRACE: the highly segmented Si-pad telescope detector modules

The TRACE detector has been recently designed for the discrimination of light charged particles both in fusion-evaporation and direct reactions with high detection efficiency ($\sim$100 msr of solid-angle coverage), high counting rate and high energy resolution. The modularity and high granularity provide the capability of being suitable for various purposes, like the identification of heavier ions up to carbon and oxygen. A detailed description can be found in Ref. [48].

Every single element of the TRACE detector consists of a double Si layer of 60 pads to form a $\Delta E$–$E$ telescope. The two layers are 200 μm- and 1 mm-thick, respectively, AC coupled with a resistivity higher than 10 kΩ/cm. The single pad has a pitch of $4\times4$ mm$^2$ covering an active area of about $20\times50$ mm$^2$, which is surrounded by a series of guard rings to limit the surface leakage current. The overall dark current is tens of nA in the case of the $\Delta E$ and few μA in the case of the $E$ detector.

A limited number of telescope modules, up to two, can presently be installed in the AGATA–PRISMA chamber with an appropriate mechanical support, as can be seen in Fig. 9. The

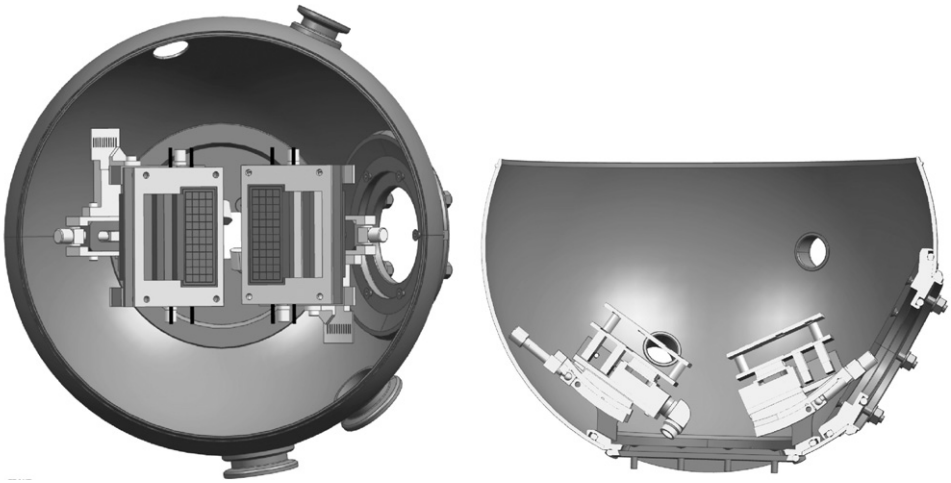

**Fig. 9.** Schematic view of two elements of the TRACE detector inside the AGATA reaction chamber. Front view (left) and top view (right).

detector can be cooled to minus tens of degrees and spans over a contained angular range with respect to the beam direction, from 8° to 26°. The angular range can be varied via a micrometer device. The angular resolution is $\sim 1^\circ$ when the cooling system is absent and $\sim 3^\circ$ otherwise.

## 6. Estimation of the performance figures of the setup by Monte-Carlo simulations

The AGATA sub-array installed at LNL is the first implementation of AGATA consisting of the first five triple clusters. The full array will consist of 60 triple cluster in a $4\pi$ geometry [2,3]. Therefore, the solid-angle coverage for the AGATA at LNL is $\frac{1}{3}\pi$ sr. In order to increase its efficiency it is possible to operate the array a distances closer than the nominal 235 mm. Consequently, its performance figures will depend in a critical way on its location relative to the target position. Detailed information on the AGATA Monte-Carlo simulations and the foreseen performance figures, for the sub-array of AGATA and the full AGATA, are published in Ref. [35]. In this section the simulations of the performance of the AGATA sub-array coupled to the PRISMA spectrometer will be discussed.

### *6.1. Simulation of the AGATA sub-array coupled to the PRISMA spectrometer*

In this section, the Doppler correction capabilities of the AGATA detectors when coupled to the PRISMA spectrometer will be evaluated in a way as realistic as possible. As mentioned in Section 3.2, the configuration of PRISMA is a magnetic quadrupole followed by a magnetic dipole. The trajectories of individual ions entering the spectrometer are software reconstructed on an event-by-event basis by exploiting the information provided by position-sensitive detectors located close to the target position and at the focal plane. Rather than implementing the geometry of PRISMA within the main simulation code for AGATA, a stand-alone simulation was developed [49,50,51].

A detailed map of the magnetic field inside the quadrupole was calculated through finite elements methods. The over-relaxation method [52] has been applied on a rectangular three-dimensional lattice, big enough to contain the whole magnet (whose inner dimensions are $32 \times 32 \times 50\ \mathrm{cm}^3$) and the mirror plate. This lattice was $100 \times 100\ \mathrm{cm}^2$ large, at the base, and 150 cm deep, and was subdivided in a cubic mesh made of $1 \times 1 \times 1\ \mathrm{cm}^3$ cells, to which were associated the values of the magnetic potential $U_m$. The relaxation method has been applied to the inner part of the magnet as well as in the fringing regions. The calculated field profile was found to be in excellent agreement with the measured field provided by the manufacturer.

Concerning the magnetic field inside the dipole, the vertical component $B_z(0)$ of the field inside the dipole was assumed to be constant on the median plane, where $B_x = B_y = 0$. The field outside the median plane could be determined in terms of $B_z(0)$ by solving the Maxwell equations. In order to treat the fringing field, the experimental values of the vertical component $B_z$ of the fringing field were fitted with a Fermi-like function. Measurements of the vertical component $B_z$ of the fringing field were available at the entrance and exit of the magnet on the median plane and at two planes, located 5 cm above and below the median plane, with 2 cm steps for the mapping. Again, $B_x$ and $B_y$ could be expressed in terms of $B_z(0)$ by solving the Maxwell equations.

Given the magnetic fields, it is possible to calculate, step-by-step, the trajectory of the ions from the target position up to the focal plane. At a distance of 50 cm after the dipole, it is assumed that the magnetic field is negligible and a straight trajectory is followed. Energy loss in the passive elements (foils, windows of the gas detectors) is evaluated through stopping power calculations based on the Ziegler subroutines [53]. The distribution of charge states after the target is calculated following the model described in Ref. [54].

The simulation codes for AGATA and PRISMA can both decode the same input event file. The output of the two programs can be combined into a single data file, based on the event number. This process closely mimics the behavior of the actual AGATA+PRISMA data acquisition system.

The example presented here considers a very schematic event generation, namely $^{90}$Zr with an average energy of 350 MeV, i.e. $v/c = 9.1\%$, and a Gaussian energy dispersion with FWHM = 70 MeV. In this simulation each $^{90}$Zr emits a single 1 MeV photon. The data analysis, however, has been performed with the same techniques as used with real data.

It is clear that, in order to perform the Doppler correction, the sole information on the direction of the ions is not sufficient and the full PRISMA information should be used. This is clearly proven by the plot shown in Fig. 10 (top panel), where the same simulated dataset, considering the sub-array of AGATA at the closest distance of 145 mm from the target is analyzed in different ways. Discarding completely the information from PRISMA, that is using an average value for both velocity direction and modulus, the peak FWHM is 9.7 keV. A value of 7.4 keV is obtained when the direction is deduced from the PRISMA data on an event-by-event basis and finally a value of 2.9 keV, very close

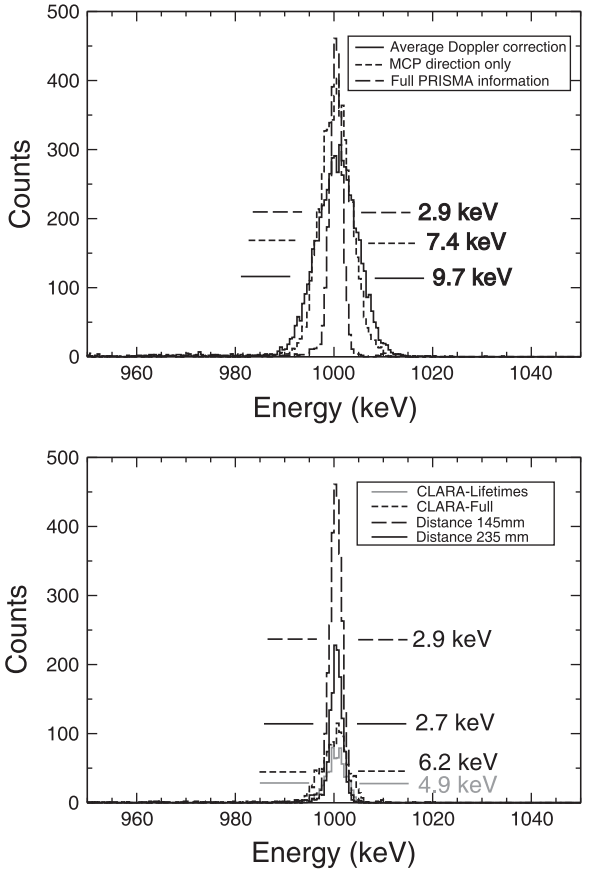


**Fig. 10.** Simulated data for the AGATA sub-array + PRISMA setup for $^{90}$Zr recoils with an average energy of 350 MeV ($v/c = 9.1\%$) and a Gaussian energy dispersion with FWHM = 70 MeV. Recoiling nuclei emitting a single 1.0 MeV photon has been simulated. In the upper panel, the simulation has been performed with the AGATA detectors placed at 145 mm from the target, the Doppler correction was performed by assuming an average recoil vector velocity modulus and taking the direction from the start detector of PRISMA (MCP detector only), or by using the full information provided by PRISMA. In the lower panel a comparison between the AGATA sub-array and the CLARA escape-suppressed array is shown. For the CLARA simulation the Doppler corrected spectra has been done with and without the 90° ring, which was the configuration for lifetimes measurements. For the AGATA sub-array simulation the Doppler correction was performed by using the full information provided by PRISMA at two target-detector distances, i.e. the nominal 235 mm and the closest 145 mm.

to the intrinsic detector resolution, is obtained by considering the full information provided by PRISMA.

The simulated performance of the AGATA sub-array and of the CLARA escape-suppressed array [9] are compared in Fig. 10 (bottom panel). The peak FWHM obtained with CLARA, considering the full information provided by PRISMA, is 6.2 keV when considering the full array and 4.9 keV when the detectors positioned at 90° with respect to the entrance of PRISMA are not considered. The value obtained with the AGATA sub-array at the "nominal" distance (235 mm from the target) is 2.7 keV, while, as discussed earlier, moving the detectors around 10 cm closer to the target position the FWHM is 2.9 keV. The slight loss in quality of the spectra is, however, compensated by the increase in photopeak efficiency of almost a factor 2.

### 6.2. Monte-Carlo simulations of the setup for RDDS measurements with grazing reactions

Recently it has been proven [25–27,45,55] that differential RDDS measurements in a setup coupling a γ-ray Ge array and a magnetic spectrometer allow to measure lifetimes of neutron-rich nuclei populated via multi-nucleon transfer or deep-inelastic reactions, which were up to now inaccessible by the conventional reactions with stable beams. The simulation of the RDDS technique for the AGATA sub-array and PRISMA setup requires an event generator capable to produce realistic events for the above mentioned experimental conditions. Those events are processed separately by the AGATA and PRISMA simulations and the results merged together on an event-number basis to be further analyzed. A comparison between experimental data from $^{48}$Ca (310 MeV) on $^{208}$Pb reaction [25] and simulated data for the same reaction can be found in Ref. [26].

The events are generated randomizing the exponential law governing the de-excitation of the levels and considering the lifetime as an input parameter. For a randomly extracted time of emission, the velocity vector, together with the energy of the γ transition are written into a file, to be used as input of the AGATA simulation. For the same event the velocity vector after the degrader is written into another file to be used as well as input of the PRISMA simulation. To speed up the Monte-Carlo simulation, the energy loss is calculated and stored in the initialization phase. This is possible when the energy loss per unitary path is constant and the energy is well above the Bragg peak.

The generator considers that the cross-section of the reaction products is constant within the angular acceptance of PRISMA, centered at the grazing angle of the reaction. The velocity distribution of the ions, before the degrader, is deduced from the experimental distribution, obtained by the PRISMA magnetic spectrometer, when accounting for the stopping power in the degrader material using the Ziegler [53] expression for the energy loss. The energy shift between the centroids of the distributions before and after the degrader is a consequence of the energy loss of the ions in the degrader itself, which leads to a different Doppler shift for the γ-rays emitted before or after the degrader. The centroid shift determines the effective degrader thickness and represents an independent check for the angle of rotation of the plunger device with respect to PRISMA.

For each experiment the thickness of the degrader is calculated such that the energy shift between peaks, originating from the

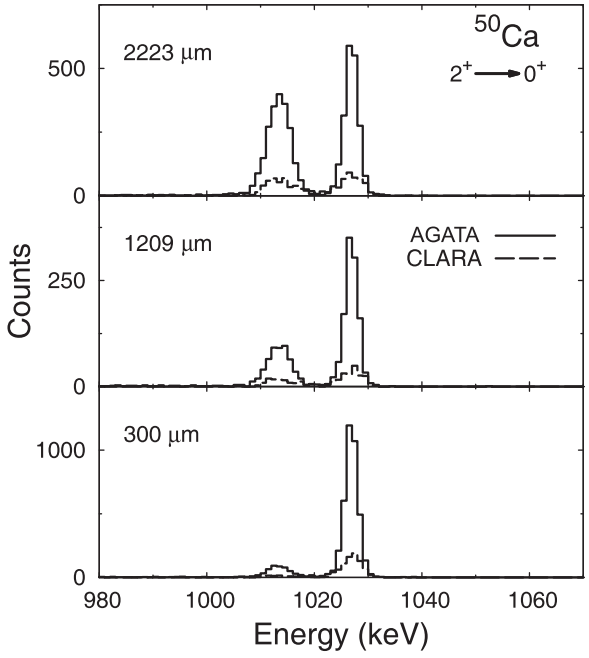


**Fig. 11.** Comparison of the RDDS simulations for the $^{50}$Ca nucleus for various distances with the AGATA sub-array and the CLARA setup coupled to the PRISMA spectrometer.

emission before and after the degrader, is larger than the energy resolution of the peak of interest as detected by the AGATA sub-array.

In addition, a realistic velocity distribution is important to determine the relative shape of the $\gamma$ transitions, which could lead to an asymmetric peak with a prominent tail [27]. This can be relevant to extend the sensitivity, via the use of reliable simulations, of the RDDS technique in the measurement of lifetimes in the range below 1 ps.

An overall comparison between simulated data sets, produced from the same input files but processed considering the AGATA sub-array and the CLARA array alternatively, is shown in Fig. 11. From the comparison at around 1 MeV, the efficiency of the AGATA sub-array is a factor 4.7 larger than CLARA and the resolution is a factor 1.4 better.

## 7. Summary

The installation of the AGATA $\gamma$-ray spectrometer, consisting of an array of five triple clusters, coupled to the PRISMA magnetic spectrometer has been concluded at INFN - Laboratori Nazionali di Legnaro (LNL). The AGATA sub-array and the PRISMA setup is ideally suited for studies of moderately neutron-rich nuclei, populated in multi-nucleon transfer and deep-inelastic reactions. In addition, RDDS lifetime measurements with the IKP-University of Cologne Plunger, will open important new perspectives for the measurement of lifetimes in neutron-rich nuclei, which were up to now inaccessible by standard experimental techniques in stable beam facilities. A number of complementary detectors, such as the heavy-ion DANTE detector, the $\gamma$-ray detector array HELENA and the highly segmented Si-pad telescope TRACE, will permit the use of AGATA for a broad range of experimental topics at LNL.

## Acknowledgments

The authors are grateful to the AGATA and PRISMA Collaborations. This work has been supported by the Istituto Nazionale di Fisica Nucleare (Italy), by the Science and Technology Facilities Council (UK) and by BMBF, Germany, under Grants 06K-167 and 06KY205I. A.G. and E.F. acknowledge the support of MICINN, Spain, and INFN, Italy through the ACI2009-1070 bilateral action. A.G. activity has been partially supported by the MICINN and Generalitat Valenciana, Spain, under grants FPA2008-06419 and PROMETEO/2010/101.

## References

[1] The AGATA Collaboration, Nucl. Instr. and Meth., in preparation.
[2] D. Bazzacco, on behalf of the AGATA Collaboration, Nucl. Phys. A 746 (2004) 248.
[3] I.-Y. Lee, J. Simpson, Nucl. Phys. News Int. 20 (2010) 23.
[4] J. Simpson, on behalf of the AGATA Collaboration, J. Phys. G: Nucl. Part. Phys. 31 (2005) S1801.
[5] G. Fortuna, et al., Nucl. Instr. and Meth. A 287 (1990) 253.
[6] A. Lombardi, et al., in: Proc. Particle Accelerator Conference, Vancouver, Canada, 1997.
[7] A. Wiens, et al., Nucl. Instr. and Meth. A 618 (2010) 223.
[8] A. Stefanini, et al., Nucl. Phys. A 701 (2002) 217c.
[9] A. Gadea, et al., Eur. Phys. J. A 20 (2004) 193.
[10] P.-A. Söderström, et al., Nucl. Instr. and Meth. A 638 (2011) 96.
[11] R.S. Kempley, et al., INFN-LNL Report, vol. 230, 2010, p. 17.
[12] F. Recchia, et al., INFN-LNL Report, vol. 230, 2010, p. 53.
[13] J.J. Valiente-Dobón, et al., INFN-LNL Report, vol. 230, 2010, p. 61.
[14] R. Nicolini, et al., INFN-LNL Report, vol. 230, 2010, p. 65.
[15] M.W. Guidry, et al., Phys. Lett. B 163 (1985) 79.
[16] R. Broda, et al., Phys. Lett. B 251 (1990) 45.
[17] R. Broda, et al., Phys. Rev. Lett. 74 (1995) 868.
[18] A. Hodsdon, et al., Phys. Rev. C 75 (2007) 04313.
[19] X. Liang, et al., Phys. Rev. C 74 (2006) 04311.
[20] B. Fornal, et al., Phys. Rev. C 77 (2008) 014304.
[21] S. Lunardi, et al., Phys. Rev. C 76 (2007) 034303.
[22] J.J. Valiente-Dobón, et al., Phys. Rev. C 78 (2008) 024302.
[23] N. Marginean, et al., Phys. Lett. B 33 (2006) 696.
[24] E. Sahin et al., private communication.
[25] J.J. Valiente-Dobón, et al., Phys. Rev. Lett. 102 (2009) 242502.
[26] D. Mengoni, et al., Eur. Phys. J. A 4 (2009) 387.
[27] D. Mengoni, et al., Phys. Rev. C 82 (2010) 024308.
[28] R. Venturelli, D. Bazzacco, LNL-NFN (Report), vol. 204, 2005, p. 220.
[29] A. Olariu, et al., IEEE Trans. Nucl. Sci. NS-53 (2006) 1028.
[30] F.C.L. Crespi, et al., Nucl. Instr. and Meth. A 570 (2007) 459.
[31] F.C.L. Crespi, et al., Nucl. Instr. and Meth. A 604 (2009) 604.
[32] J. Van der Marel, B. Cederwall, Nucl. Instr. and Meth. A 437 (1999) 538.
[33] A. Lopez-Martens, et al., Nucl. Instr. and Meth. A 533 (2004) 454.
[34] Th. Kröll, D. Bazzacco, Nucl. Instr. and Meth. A 565 (2006) 691.
[35] E. Farnea, et al., Nucl. Instr. and Meth. A 621 (2010) 331.
[36] G. Montagnoli, et al., Nucl Instr. and Meth. A 547 (2005) 455.
[37] J.J. Valiente-Dobón, et al., Acta Phys. Pol. B 37 (2006) 225.
[38] A. Gottardo, et al., Nucl. Phys. A 805 (2008) 606c.
[39] E.M. Kozulin, et al., Heavy Ions Physics Scientific Report (JINR, FLNR) Dubna (1995–1996), p. 215.
[40] A. Maj, et al., Nucl. Phys. A 571 (1994) 185.
[41] M. Mattiuzzi, et al., Nucl. Phys. A 612 (1997) 262e.
[42] Th. Pissula, A. Dewald, J. Jolie, Nucl. Instr. and Meth. A, to be published.
[43] A. Dewald, et al., The 98 Seminar on Nuclear Physics with Radioactive Ion Beam and High Spin Nuclear Structure, Lanzhou, China, in: G. Jin, Y. Luo, W. Zhan (Eds.), Atomic Energy, Beijing, 1998.
A. Dewald, in: Ancillary Detectors and Devices for Euroball, H. Grawe (Ed.), GSI and the Euroball Ancillary Group, Darmstadt, 1998, p. 70.
[44] T. Pissulla, Diploma Thesis, Institute for Nuclear Physics, University of Cologne, 2008.
[45] J. Ljungvall, et al., Phys. Rev. C 81 (2010) 061301.
[46] H. Savajols, et al., Nucl. Phys. A 654 (1999) 1027c.
[47] J. Simpson, et al., Heavy Ion Phys. 11 (2000) 159.
[48] D. Mengoni, Ph.D. Thesis, Università di Camerino, 2006.
[49] A. Latina, Ph.D. Thesis, Università di Torino, 2006.
[50] D. Montanari, Ph.D. Thesis, Università di Milano, 2010.
[51] D. Montanari, et al., Eur. Phys. J. A 47 (2011).
[52] S. Humphries, Principles of Charged Particle Acceleration, John Wiley and Sons, Ltd., 1999.
[53] J.F. Ziegler, J. Appl. Phys. 31 (1977) 544.
[54] R.O. Sayer, Rev. Phys. Appl. 12 (1972) 1543.
[55] A. Gadea, et al., Acta Phys. Pol. B 38 (2007) 1311.